

Time variable Earth's gravity field from SLR and GNSS satellites

International Association of Geodesy
Scientific Assembly 2013
September 1–6, 2013, Potsdam, Germany

Introduction

GPS satellites are very sensitive to some of the Earth's gravity field coefficients, because of the deep 2:1 orbital resonance. The resonant coefficients (C_{22} , S_{22} , C_{32} , S_{32} , C_{44} , S_{44}) cause a secular drift of the semi-major axes up to 5.3 m/day (Hugentobler 1998). We processed 10 years of GPS and GLONASS data using the standard orbit modeling from the Center of Orbit Determination in Europe (CODE) with a simultaneous estimation of the Earth gravity field coefficients and other parameters (Tab. 1). The weekly GNSS solutions are compared to weekly SLR and monthly GRACE gravity field solutions.

Figure 2 shows the amplitudes of annual signals of gravity field coefficients from the GNSS, SLR, and GRACE solutions. The median differences are 0.11, 0.12, and $0.09 \cdot 10^{-10}$ between GNSS-GRACE, GNSS-SLR, and SLR-GRACE, respectively. The mean amplitude in all solutions is $0.28 \cdot 10^{-10}$, i.e., the amplitudes agree on average at the 30% level.

Figure 3 shows that the sectorial and tesseral coefficients agree very well in the SLR and GRACE solutions, whereas the zonal terms show large deviations:

- > variations of C_{20} are overestimated in the GRACE solutions (Fig. 2), because of the alias with S_2 tide (Meyer et al., 2012). C_{20} from the GNSS solutions does not fully agree with the SLR results, but can be improved by changing the orbit modeling (see Sec. 1),
- > C_{30} agrees in the GRACE and GNSS solutions and disagrees in the SLR solution (Fig. 3), because of the correlations between C_{30} and C_{50} in the SLR solution using 5 spherical satellites (see Sec. 2),
- > C_{40} agrees in the SLR and GNSS solutions, and disagrees in the GRACE solution, because of the alias with S_2 tide (see Sec. 2).

1. Earth's Gravity Field from GPS and GLONASS

Figure 4 shows that the variations of C_{20} do not seem to be fully recovered from the standard CODE orbit parametrization, which is reflected in substantially smaller amplitudes of annual and semiannual signals as compared to the SLR solutions. Figure 5 shows that C_{20} can be much better determined from the GNSS solutions if the constant and once-per-revolution parameters in the X direction are not estimated: the semi-annual signal is well reproduced, the 3rd harmonic of 118 days disappears, and the correlation coefficient between the SLR and GNSS series increases from 0.02 to 0.28. A very good agreement between SLR and GNSS solutions is observed in particular for the period after 2008 when the contribution of GLONASS satellites becomes prominent and the GLONASS-observing network becomes more global. It is important to avoid the estimation of both constant X and once-per-rev orbit parameters in the X direction, because both parameters are correlated with C_{20} and all solutions with estimating one of these parameters or both show similar results with the inappropriate C_{20} estimates (as in Fig. 4).

The spectral analysis shows the 2nd, 3rd, 4th, 5th, and 7th harmonics of the draconitic year in most of the GNSS-derived coefficients (Fig. 4-5, Fig. 7-8). The amplitudes of these harmonics can be reduced for some parameters when not estimating X_0 , X_s , X_c (see Fig. 8). The quality of other estimated parameters, e.g., ERPs and station coordinates, are, however, degraded when X_0 , X_s , X_c are not estimated.

The standard errors of GNSS-derived gravity field coefficients are much smaller for degree 2 and for the GPS resonant coefficients than for the remaining coefficients (Fig. 6). The errors of coefficients of degree 2 are at the same level in the GNSS, GRACE, and SLR solutions. The a posteriori errors of GPS resonant coefficients (Fig. 7) are too optimistic in the GNSS solutions, because the resonant terms are correlated with the solar radiation pressure to a greater extent than non-resonant terms, and thus, strongly affected by modeling issues.

- The correlation matrix (Fig. 9) shows the correlations between:
- > UT1-UTC & C_{20} & C_{40} & osculating elements (A, i, Ω),
 - > Z, X, Y geocenter coordinates & C_{30}, C_{31}, S_{31} , respectively,
 - > D_0 & $S_{22}/C_{22}, S_{32}/S_{32}, C_{44}/S_{44}$ (resonant terms),
 - > C_{20} & X_0 .

2. Earth's Gravity Field from SLR

Most of the low degree Earth's gravity field coefficients can be determined from the multi-SLR solutions (LAGEOS-1, LAGEOS-2, AJISAI, Starlette, Stella) with a comparable quality to the GRACE solutions (Fig. 10). C_{20} and C_{40} are better defined in the SLR solutions, because of the alias with S_2 tide in the GRACE solutions (Fig. 11, top). On the other hand, C_{30} cannot be fully recovered from the SLR solution (Fig. 11, bottom), because C_{30} and C_{50} impose similar orbit perturbations on low orbiting SLR satellites, i.e., on Starlette, Stella, and AJISAI (Cheng et al., 1997). Thus, a lumped coefficient $C_{30}+0.9 \cdot C_{50}$ is derived from the SLR solutions, instead. Some of the coefficients from the multi-SLR solutions are affected by the mismodeling of the solar radiation pressure (e.g., C_{41} in Fig. 12), because their spectral analyses show periods related to a draconitic year of Starlette (73 days) and AJISAI (89 days), or Starlette's revolution of perigee (121 days).

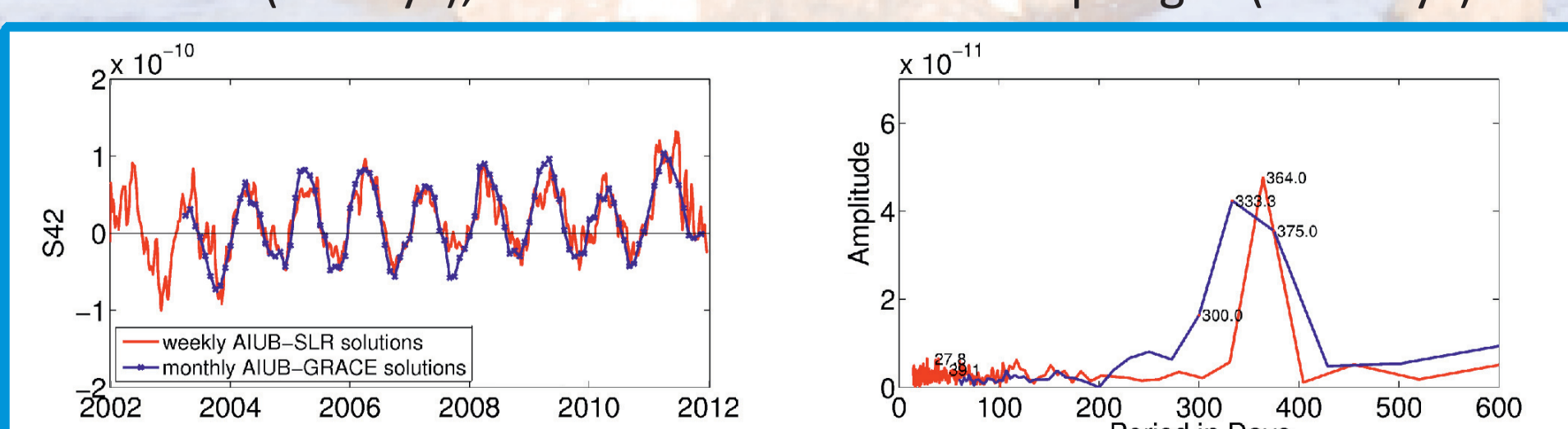


Fig. 10: Variations of C_{42} w.r.t. EGM2008 from the SLR solutions using 5 spherical satellites compared to the GRACE results. 4-week low-pass filter is applied to the SLR results

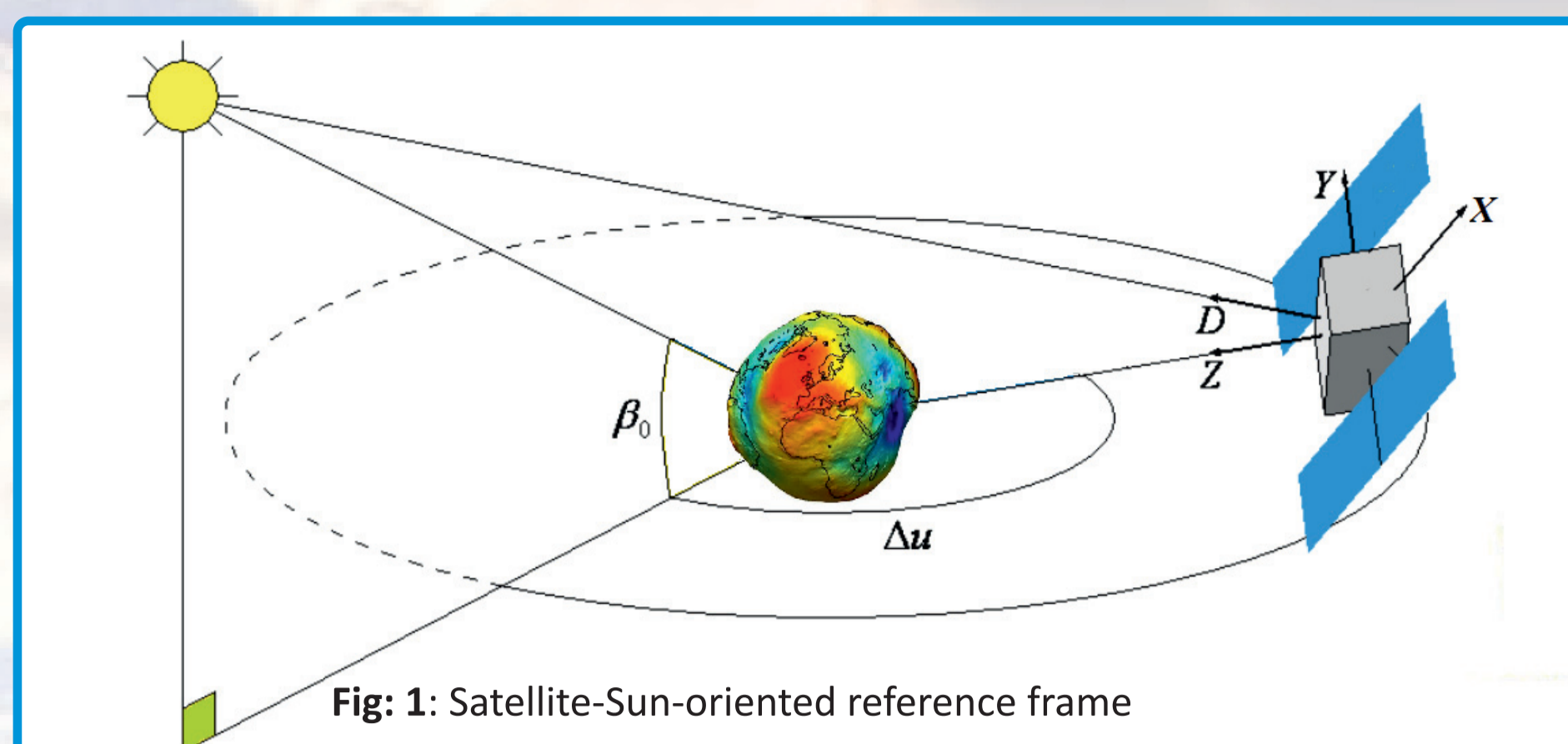


Fig. 1: Satellite-Sun-oriented reference frame

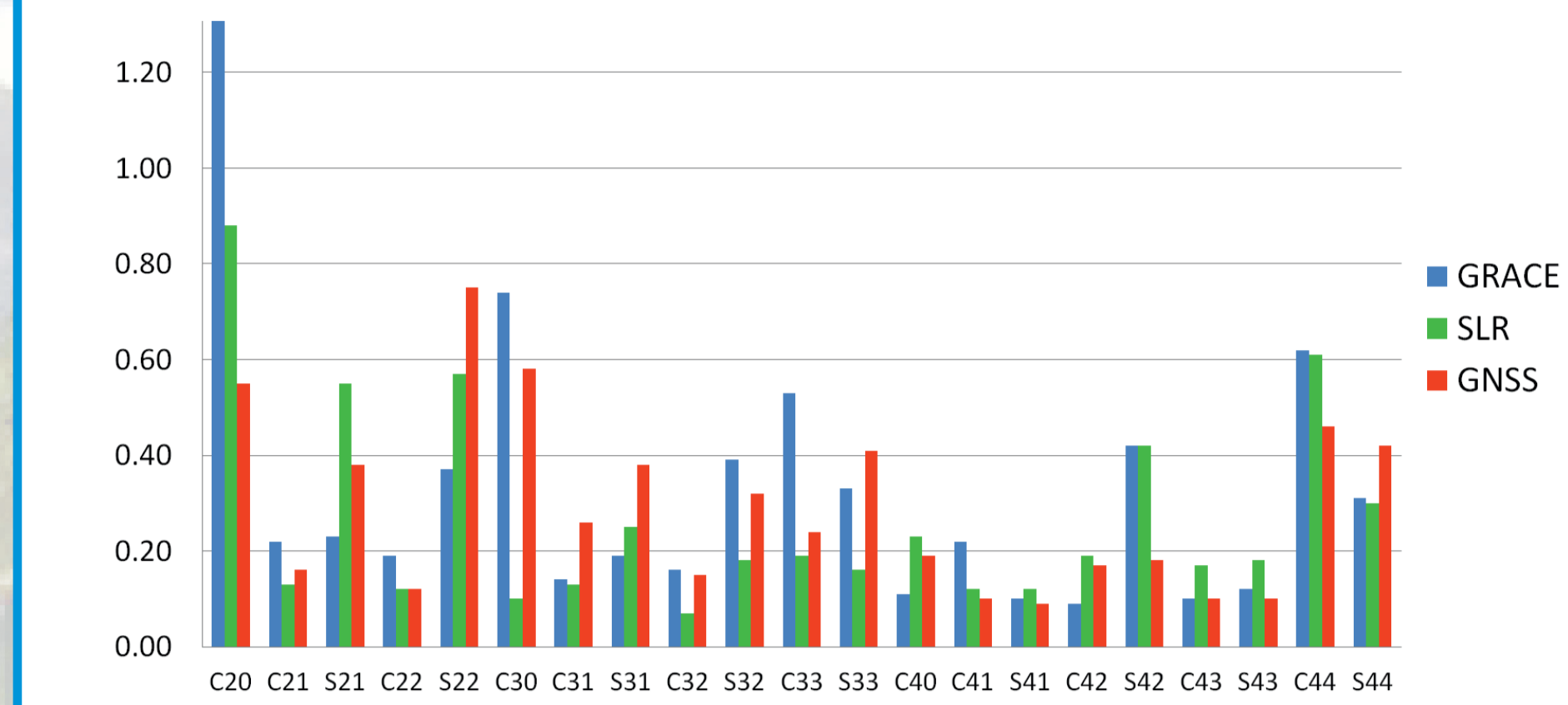


Fig. 2: Amplitudes of annual signals of gravity field coefficients ($\cdot 10^{-10}$) estimated using a posteriori fit

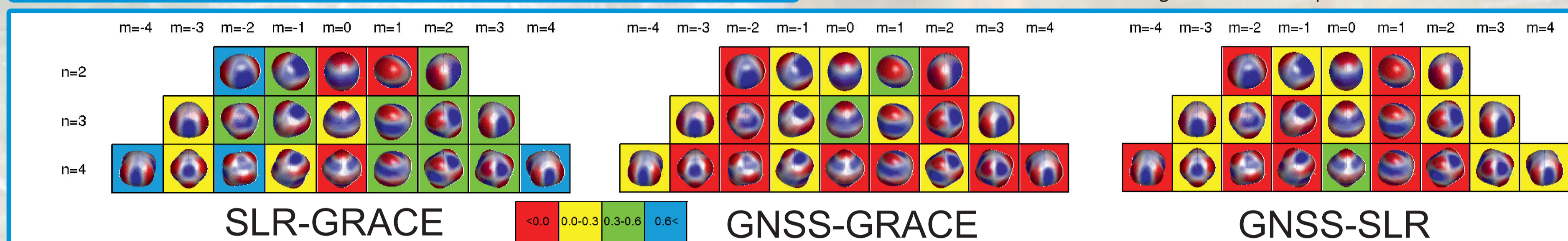


Fig. 3: Correlations between Earth gravity field coefficient variations from the SLR, GRACE, and GNSS solutions (with standard CODE orbit modeling). Correlation coefficients were estimated using the series of the 7-day SLR and 7-day GNSS solutions, and interpolated values of monthly GRACE solutions with subtracting the mean value of each series.

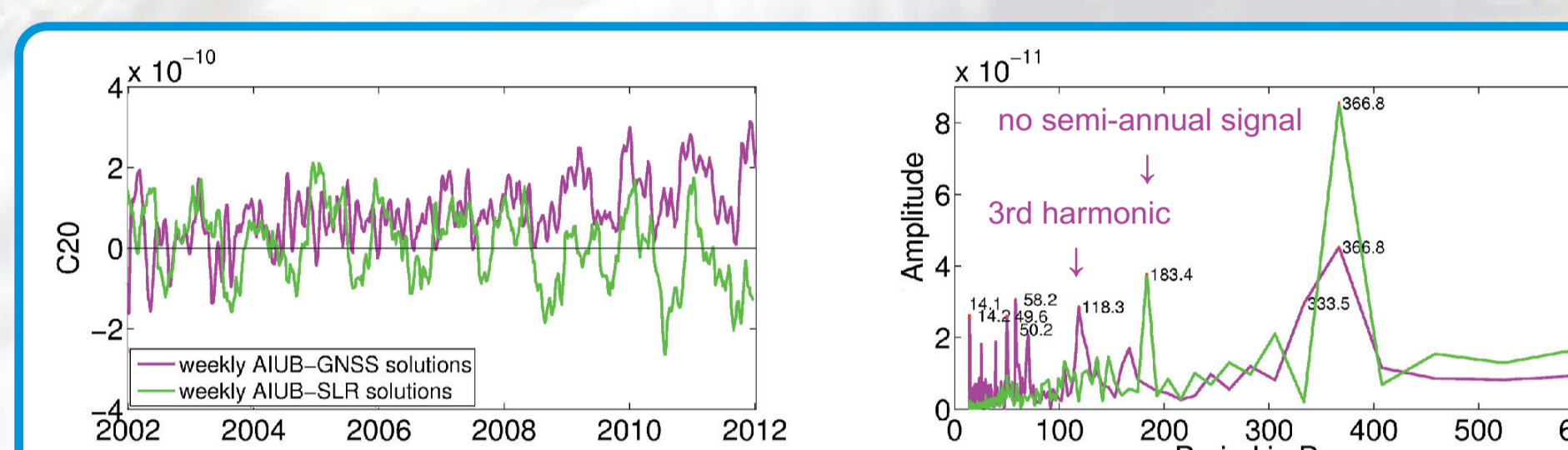


Fig. 4: Variations of C_{20} w.r.t. EGM2008 from the GNSS solutions with standard CODE modeling, compared to the SLR results for a time span 2002-2011

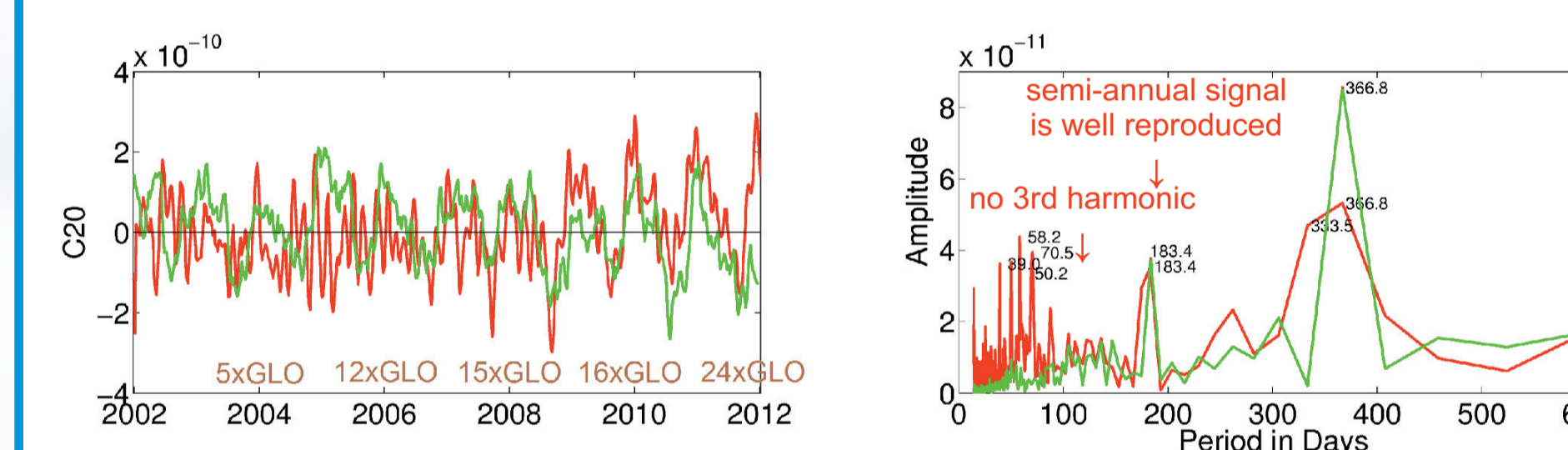


Fig. 5: Variations of C_{20} w.r.t. EGM2008 from the GNSS solutions without estimating constant and once-per-rev dynamical orbit parameters in the X direction, compared to the SLR results

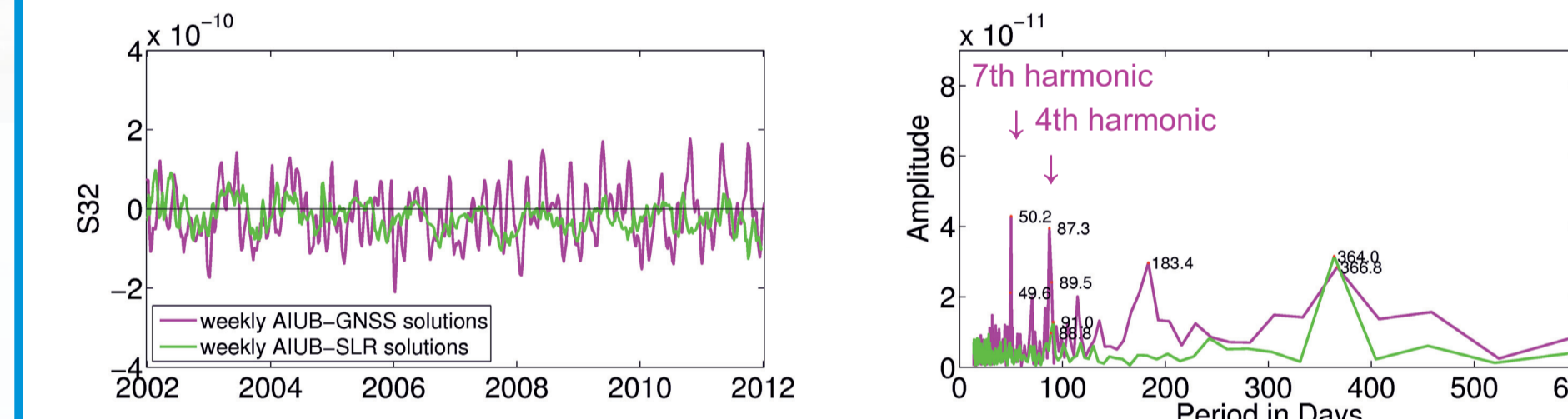


Fig. 7: Variations of S_{32} resonant term from the GNSS solutions using standard CODE modeling

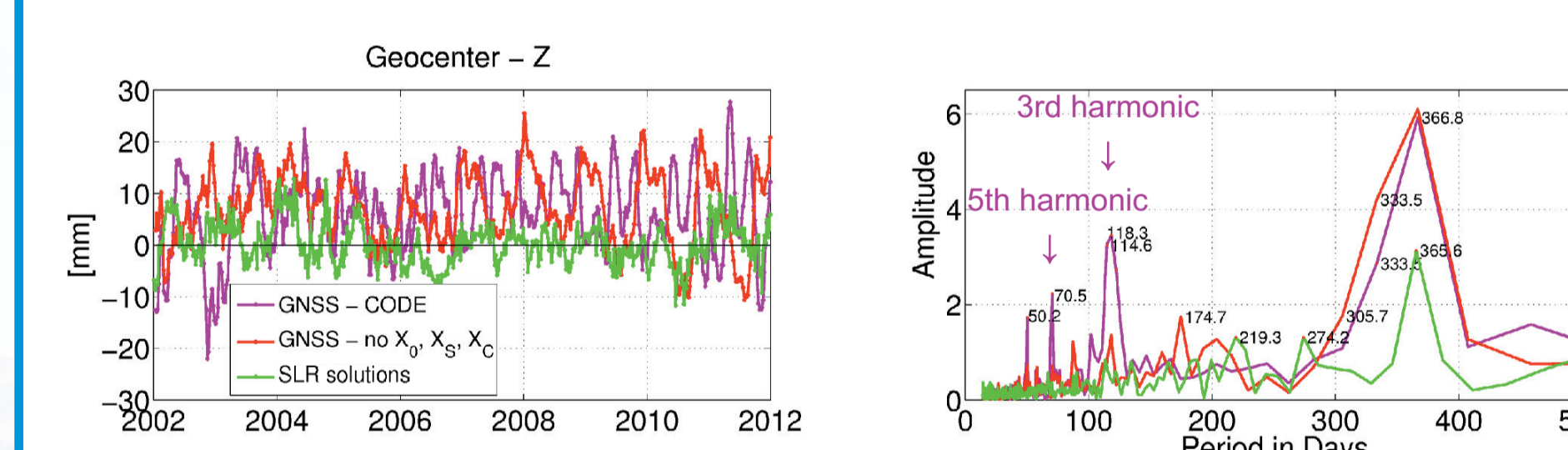


Fig. 8: Z geocenter coordinate from the SLR solutions and the GNSS solutions with standard CODE modeling and without estimating constant and once-per-rev dynamical orbit parameters in the X direction

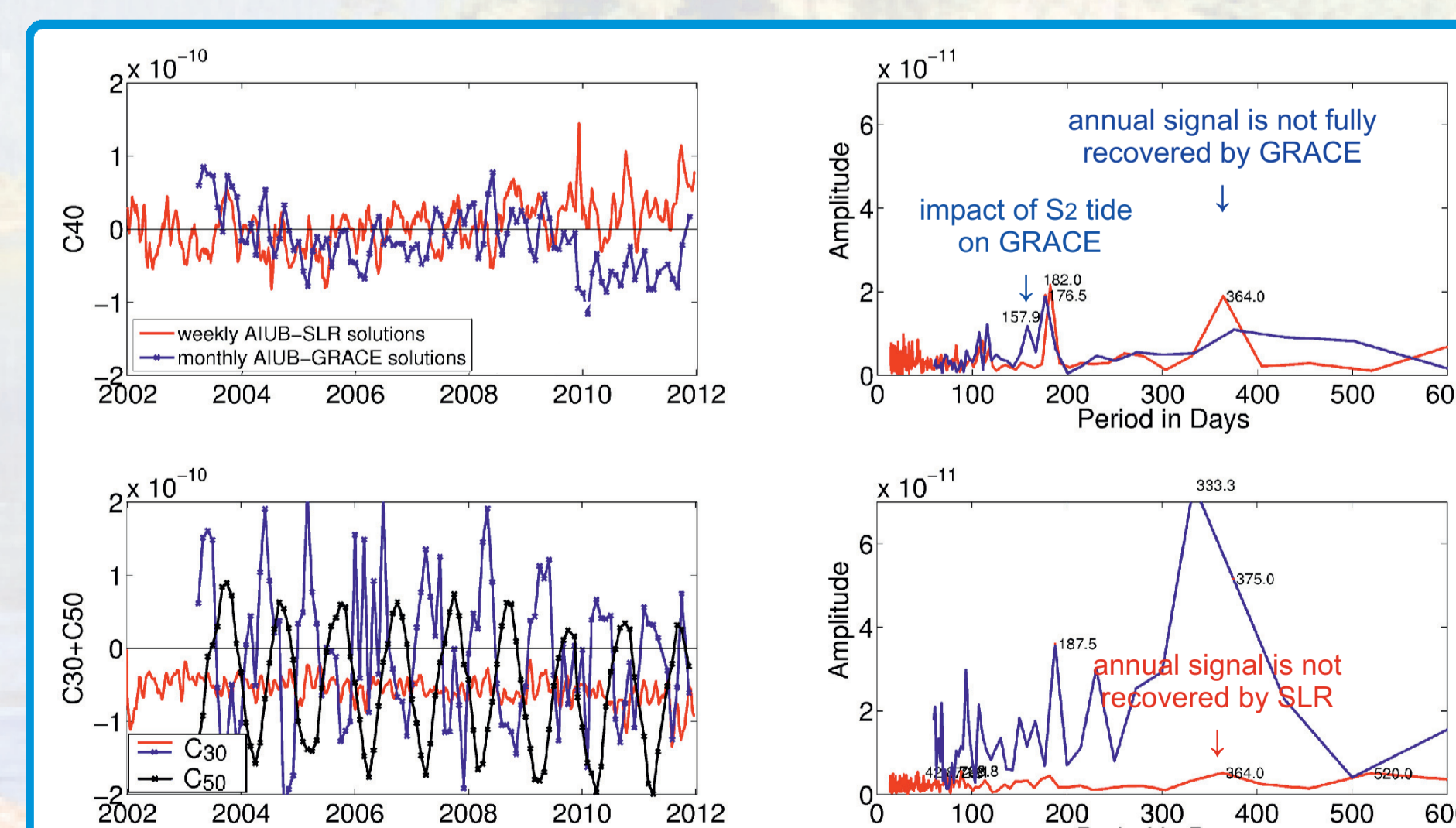


Fig. 11: Variations of C_{40} and C_{30} w.r.t. EGM2008 from the SLR solutions compared to the GRACE results. C_{50} from the GRACE solutions is also shown

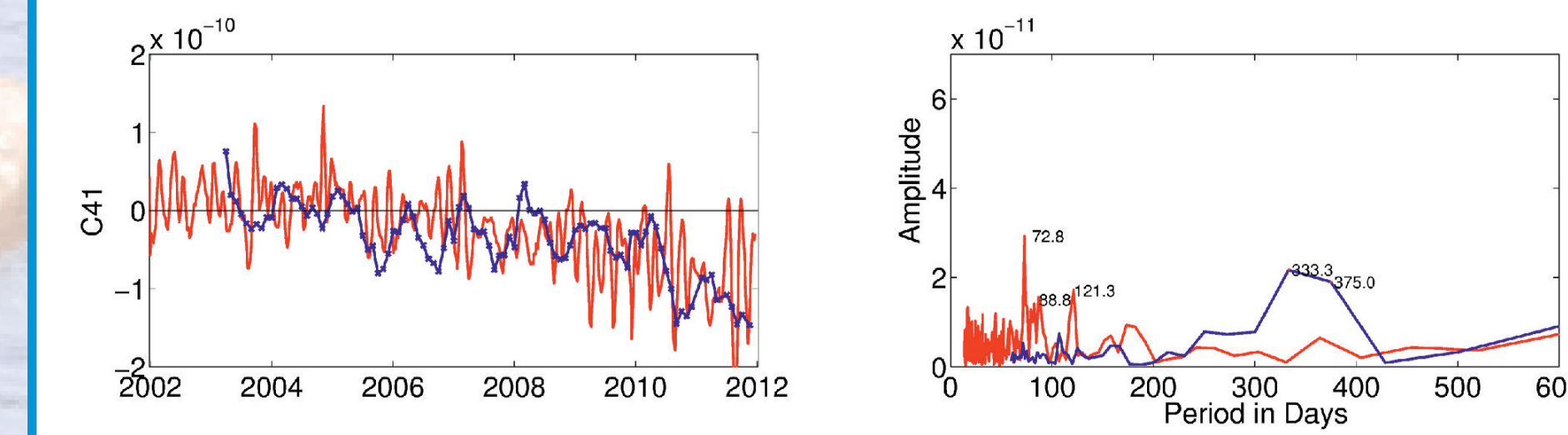


Fig. 12: Variations of C_{41} w.r.t. EGM2008 from the SLR solutions using 5 spherical satellites compared to the GRACE results

K. Sošnica¹, A. Jäggi¹, G. Beutler¹, U. Meyer¹, R. Dach¹, D. Thaller², and L. Mervart³

- ¹ Astronomical Institute, University of Bern, Bern, Switzerland
² Bundesamt für Kartographie und Geodäsie, Frankfurt am Main, Germany
³ Institute of Advanced Geodesy, Czech Technical University, Prague, Czech Republic

Estimated parameters	GNSS solutions	SLR solutions
Orbits		
Osculating elements	up to 32 GPS and 24 GLONASS satellites (1 set per 3 days)	LAGEOS-1/2, Starlette, Stella, Ajisai (1 set per 7 days)
Dynamical parameters	D_0, Y_0, X_0, X_s, X_c (1 set per 3 days, see Fig. 1)	LAGEOS-1/2: S_0, S_c, S_s (1 set per 7 days) Sta/Ste/Aji: C_p, S_c, S_s, W_c, W_s (1 set per day)
Pseudo-stochastic pulses	R, S, W (once per revolution)	LAGEOS-1/2: no pulses Sta/Ste/Aji: S (once per revolution)
Earth rotation parameters	$X_p, Y_p, UT1-UTC$ (1 set per day)	$X_p, Y_p, UT1-UTC$ (1 set per day)
Geocenter coordinates	1 set per 7 days	1 set per 7 days
Earth gravity field	Estimated up to d/o 4/4 (1 set per 7 days)	Estimated up to d/o 4/4 (1 set per 7 days)
Station coordinates	1 set per 7 days	1 set per 7 days
Other parameters	Troposphere ZD (2h), gradients (24h), GNSS-specific translations and ZTD biases	Range biases for selected stations

Tab. 1: List of estimated parameters in the 7-day GNSS and 7-day SLR gravity field solutions. The modeling standards follow the IERS 2010 Conventions in both solutions. 7-day GNSS solutions are generated by stacking seven 3-day NEQs with overlapping orbits (stacking all parameters with except for the orbits). The gravity field coefficients are derived from the GNSS solution together with other parameters for the first time.

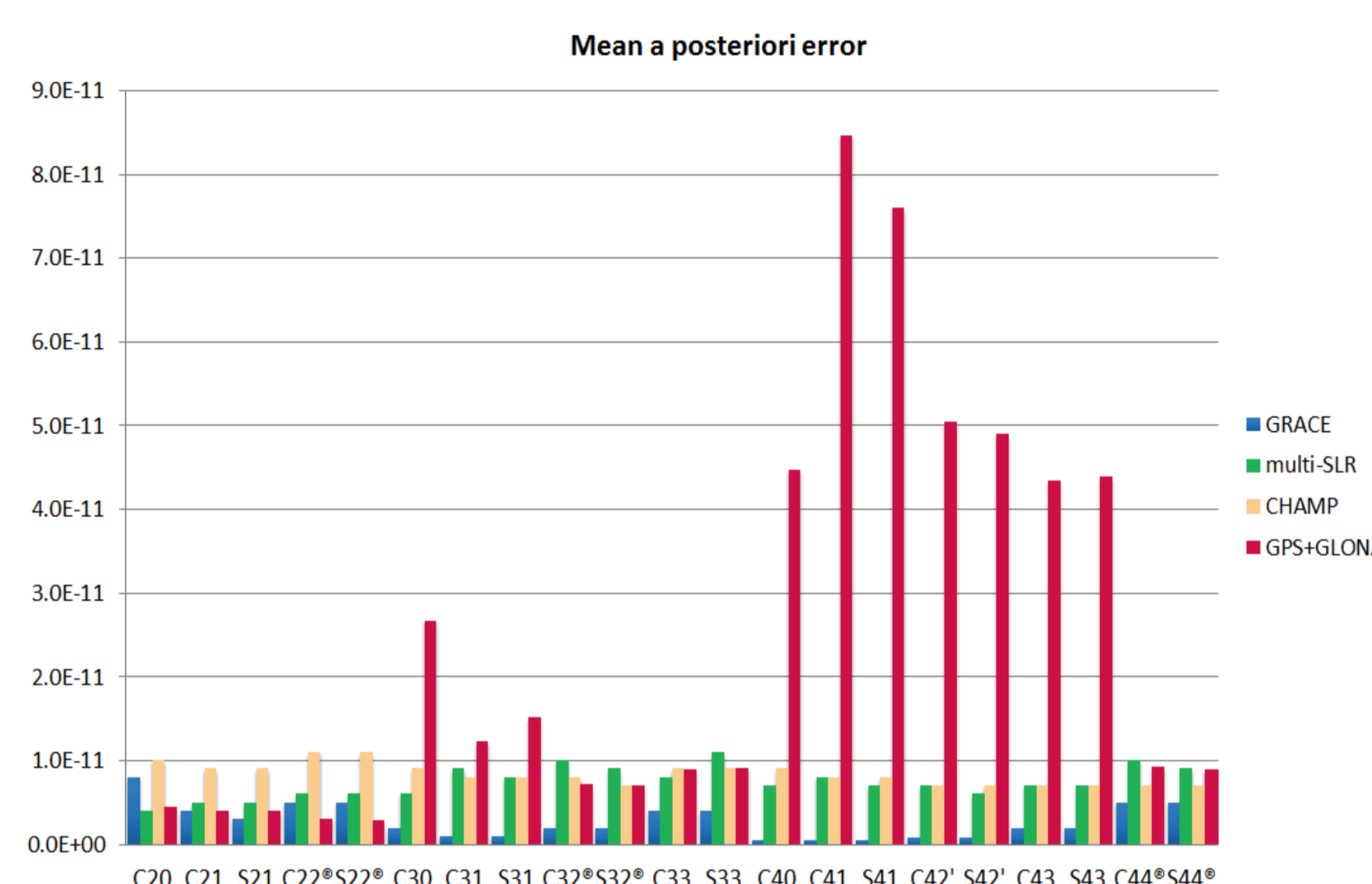


Fig. 6: Mean a posteriori errors of gravity field parameters from the GRACE, SLR, CHAMP, and GNSS solutions. GPS resonant coefficients are marked by ®

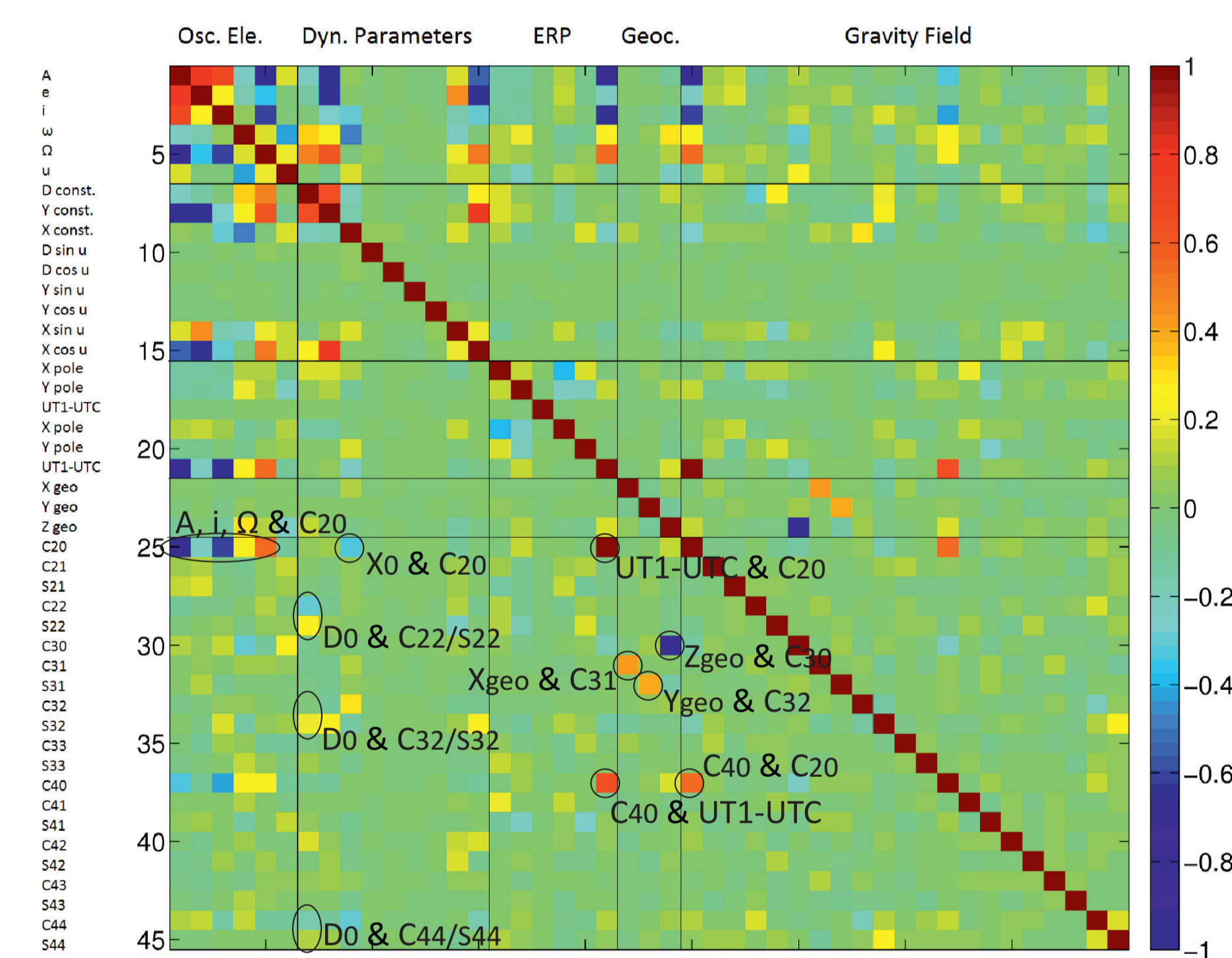


Fig. 9: Correlation matrix from reduced daily normal equation system. The osculating elements and dynamical parameters of one GPS satellite are shown with Earth rotation parameters (ERP), Geocenter coordinates and gravity field parameters

3. Summary

- > The increasing number of GLONASS satellites and a well-distributed network of GNSS stations improve the quality of the GNSS-derived C_{20} (Fig. 5).
- > C_{20} is correlated with constant and once-per-rev dynamic orbit parameters in the X direction. C_{20} can be well established from GNSS when these orbit parameters are not set up.
- > GPS resonant gravity field parameters have very small a posteriori errors, but they are strongly affected by the solar radiation pressure (correlation with D_0).
- > Most of the gravity field parameters of low degree can be well established from the SLR solutions with a comparable quality to the GRACE results. The quality of C_{20} and C_{40} is better in the SLR solutions, whereas C_{30} is better recovered in the GRACE and GNSS solutions.

References

- [1] Beutler G (2005) Methods of Celestial Mechanics. Springer-Verlag
- [2] Cheng M, Shum C, Tapley B (1997) Determination of long-term changes in the Earth's gravity field from satellite laser ranging observations. J Geophys Res, 102(B10),
- [3] Hugentobler U (1998) Astrometry and Satellite Orbits: Theoretical Considerations and Typical Applications. Geodätisch-geophysikalische Arbeiten in der Schweiz vol. 57
- [4] Neichen D, Beutler G, Hugentobler U (2003) Sensitivity of GPS and GLONASS orbits with respect to resonant geopotential parameters. J Geod vol. 77 (7-8): 478-486
- [5] Meyer U, Jäggi A, Beutler G (2012) Monthly gravity field solutions based on GRACE observations generated with the Celestial Mechanics Approach. Earth Plan Sci Lett 345(72)
- [6] Sošnica K, Thaller D, Dach R, Jäggi A, Beutler G (2013) Contribution of Starlette, Stella, and AJISAI to the SLR-derived global reference frame. Submitted to J Geod

